Random walk of liquid droplets migrating in silicon

T. R. Anthony and H. E. Cline

General Electric Corporate Research and Development Center, Schenectady, New York 12308

The dislocation-induced random walk of an aluminum-rich droplet migrating in a thermal gradient along the $\langle 100 \rangle$ axis in silicon is shown to lead to an appreciable mean square displacement of the droplet from its original $\langle 100 \rangle$ thermal trajectory over migration distances of about 1 cm. When ordered arrays of droplets are migrated to produce columnar diode arrays in silicon, this random walk causes disregistry in the arrays. The disregistry can be minimized by introducing a small off-$\langle 100 \rangle$-axis thermal gradient superimposed on the major $\langle 100 \rangle$ thermal gradient. This off-axis component of the thermal gradient overwhelms dislocation intersection effects which cause random walk and leads to a uniform *nonrandom* displacement which preserves the registry in the columnar diode arrays.

I. INTRODUCTION

The migration of a liquid droplet in a thermal gradient in a solid is caused by the dissolution of atoms of the solid on the hot side of the droplet, diffusion of the dissolved atoms across the droplet, and the subsequent deposition of the dissolved atoms of the solid on the cold side of the droplet. The rate of migration may be limited either by the diffusion rate of dissolved solid atoms across the droplet or by the atomic dissolution and deposition rates at the solid-liquid interfaces of the droplet. In this latter case, the migration rate of the droplet will be sensitive to the crystal perfection of the solid since dislocations and/or grain boundaries which intersect the droplet can significantly increase interface dissolution and deposition rates by providing a source of atomic ledges and kinks on the interfaces of the droplet. [1-3]

A droplet migrating up a thermal gradient will collide with dislocations in its path. Such intersecting dislocations will increase the dissolution or deposition rates on those droplet interfaces which they cross. With random dislocations, this selective dissolution and deposition will occur at random on the various droplet facets. For those droplet facets which are not perpendicular to the thermal gradient, such selective dissolution will cause the droplet to be randomly displaced in a direction perpendicular to the thermal gradient. A large number of sequential dislocations intersections during droplet migration will consequently result in a substantial diffusion-type displacement of the droplet perpendicular to its original path.

The random-walk displacement of migrating droplets from their thermal gradient trajectories is a technologically important problem since such displacements limit the quality of columnar diode arrays, produced by migrating a large array of aluminum-rich droplets through n-type silicon crystals[4,5] and used in electronic devices, radiation detectors and vertical-junction solar cells. In this paper, the effects of dislocation density, temperature, droplet size, and the crystallographic droplet migration direction on the random-walk displacement of aluminum-rich droplets migrating up a thermal gradient in silicon will be examined. It will be shown that such displacements can be minimized by the selection of crystals with certain dislocation density

ranges and by the appropriate choice of droplet migration directions in the silicon crystal.

II. EXPERIMENTAL PROCEDURE

Previous experience has indicated that the $\langle 100 \rangle$ direction is the most suitable droplet thermomigration direction in silicon because of such factors as droplet stability and ease of droplet penetration at the starting $\langle 100 \rangle$ vacuum-solid interface.[4-6] Consequently, $\langle 100 \rangle$ 1-in.-diam single-crystal ingots of n-type 10-Ω cm silicon containing between 10 and 10^7 dislocations/cm² were obtained for the experiments. The as-obtained crystals were sliced into 1-cm-long ingots. The faces of these ingots were polished, oxidized, and patterned by conventional photolithography and etching techniques
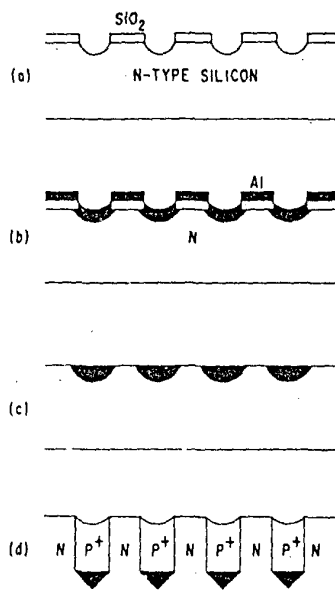

FIG. 1. Sequence of schematic diagrams showing the experimental procedure used to produce an array of aluminum-rich droplets in silicon. (a) Patterning and etching of an array of holes in a silicon matrix by photolithography and etching techniques; (b) vapor deposition of an aluminum film in holes; (c) removal of excess aluminum by polishing; (d) alloying and migration of droplets in a thermal gradient.
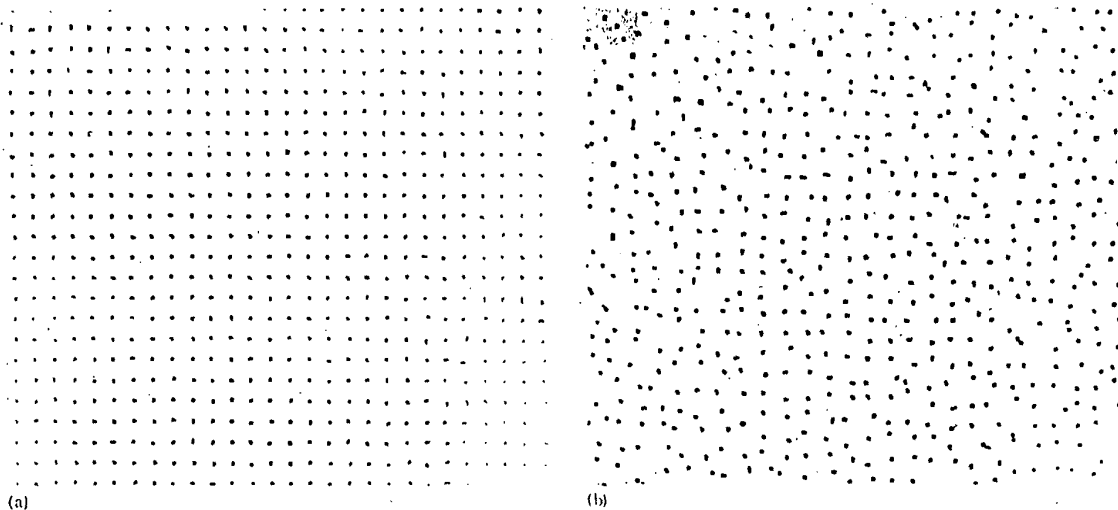
FIG. 2. (a) Wafer face where droplets entered. p-type faceted droplet trails in n-type matrix are revealed by chemical staining. Droplet array has migrated exactly along the ⟨100⟩ direction. (100×) (b) Wafer face of (a) ingot where droplets exited. Random-walk displacements of droplets perpendicular to the thermal trajectory through the wafer have caused the initially regular array to become irregular. Droplet migration was exactly along a ⟨100⟩ direction and droplet trails are faceted. (100×.)

to produce a 50×50 square array of holes 30μ deep on 20 ml centers (Fig. 1).[5] An aluminum film was deposited into the array of holes. The ingot with the patterned array of aluminum dots was then heated and subjected to a thermal gradient of 50 °C/cm. The aluminum dots alloyed with the silicon and melted to produce an array of aluminum-rich droplets which migrated up the thermal gradient and through the 1-cm-thick ingot.[5-13] The silicon redeposited behind the migrating aluminum-rich droplet was doped sufficiently with aluminum to convert the originally n-type silicon matrix to p-type silicon in

the columnar droplet trail. Experiments were carried out over a temperature range 945–1330 °C.

The ingot after thermomigration was ground and polished on both the droplet entrance [Fig. 2(a)] and exit sides [Fig. 2(b)] and the p-type trails left behind by the aluminum-rich droplets in the n-type ingots were revealed by conventional chemical staining. Twenty-five hundred interneighbor distances, X, between droplet trails on the same row for each of the fifty rows were measured on both the entrance and exit sides of each

TABLE I. The mean square displacement along one dimension, dislocation density, temperature, droplet size, droplet morphology, and droplet migration direction for the droplet arrays examined in the present investigation. All droplet arrays have migrated 1 cm through the silicon ingots.

$\langle X^2 \rangle^{1/2}$ (μ)	ρ dislocations (cm²)	T (°C)	Droplet size D (μ)	Droplet morphology	Migration direction
180	4.5×10^6	945	125	Faceted	⟨100⟩
138	2×10^5	980	192	Faceted	⟨100⟩
120	2×10^6	1128	90	Faceted	⟨100⟩
85	1×10^n	1330	250	Faceted	⟨100⟩
72	1×10^6	1330	191	Faceted	⟨100⟩
66	3.2×10^6	1075	90	Rounded	Several degrees off ⟨100⟩
55	6×10^5	1330	167	Faceted	⟨100⟩
53	6×10^5	1330	108	Rounded	Slightly off ⟨100⟩
44	4×10^4	1200	164	Rounded	Slightly off ⟨100⟩
43	3×10^6	1075	109	Rounded	Slightly off ⟨100⟩
32	3×10^6	1075	180	Rounded	Slightly off ⟨100⟩
31	3×10^6	1075	130	Rounded	Slightly off ⟨100⟩
13	2.1×10^5	1184	210	Rounded	Slightly off ⟨100⟩
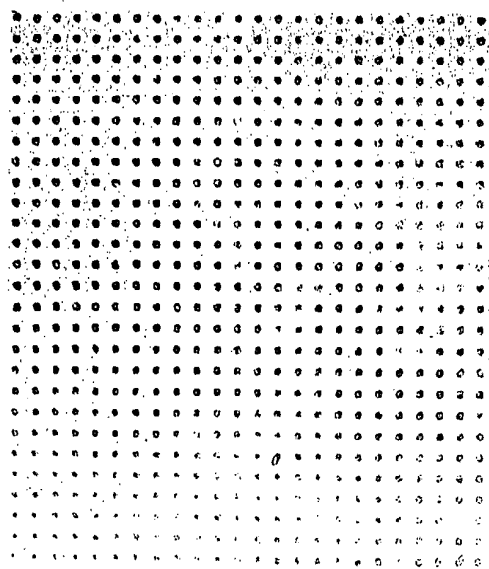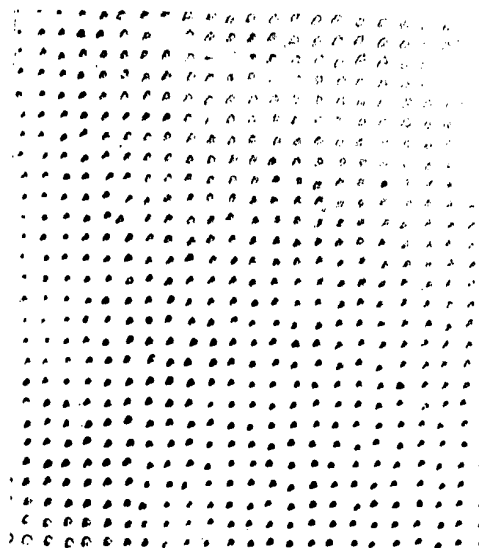
FIG. 3. (a) and (b) The entrance and exit sides of a wafer, respectively, where an array of droplets had migrated along but slightly off the (100) axis because of a slightly off-axis thermal gradient. Droplet trails are rounded and tear-drop shaped. The random-walk displacements of droplets are minimized by migrating slightly off the (100) axis as can be seen by comparing with Figs. 2(a) and 2(b), where droplets migrated exactly along the (100) direction. (105×.)

ingot and the mean square displacements $\langle X^2 \rangle$ resulting from random walk of the droplets away from their thermal gradient trajectories were determined from Eq. (1).

$$\langle X^2 \rangle = \frac{\langle X_f - \langle X_f \rangle \rangle^2}{2} - \frac{\langle X_i - \langle X_i \rangle \rangle^2}{2} . \qquad (1)$$

where X_i and X_f are respectively the interneighbor distances on the initial (entrance) and final (exit) sides of the ingot. Because the droplet array was deposited on the entrance side by photolithography techniques, the initial entrance side disregistry of the array $\langle X_i - \langle X_i \rangle \rangle^2$ was negligible and could be ignored in comparison to the exit side disregistry $\langle X_f - \langle X_f \rangle \rangle^2$ resulting from the random walk of the migrating droplets. The denominator of 2 in Eq. (1) accounts for the fact that we are measuring the interneighbor distance between two randomly walking objects and not simply the distance of a single randomly walking droplet from a fixed reference trajectory. In Table I, the random-walk displacement $(\langle X^2 \rangle)^{1/2}$ is listed in order of decreasing displacement for the various conditions listed. Also, an estimate of the number of displacements N experienced by a droplet and the average displacement step S was obtained by sectioning the sample parallel to the columnar droplet trails and examining these doped trails with an infrared transmission microscope. In addition to the experiments listed in Table I, droplet migration studies were also carried out in crystals which had been mechanically deformed 1% at 1100 °C to produce a high dislocation density (~10^6 disl/cm²) and in several crystals with a low dislocation density (10^1 disl/cm²). Dislocation densities were measured in the bulk silicon

crystal after droplet migration with Sirtl etch, a dislocation etch for silicon.

III. EXPERIMENTAL RESULTS

The most striking experimental result is that droplets migrating exactly along the (100) direction suffer relatively large mean square displacements [Figs. 2(a) and 2(b)] as compared to droplets migrating slightly off the (100) axis [Figs. 3(a) and 3(b)]. The doped trails of droplets migrating exactly on the (100) are faceted
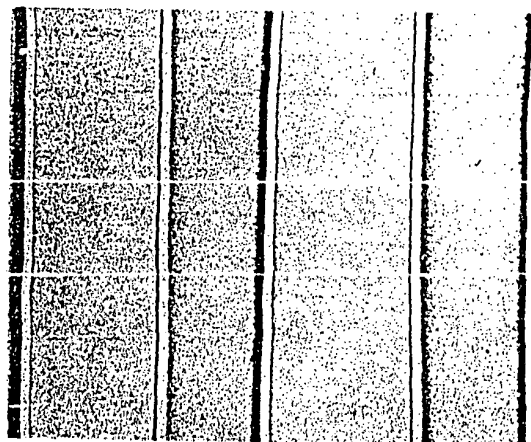

FIG. 4. Longitudinal section of a droplet trail in silicon with a low dislocation density of 50 disl/cm². Trails in such material are generally straight. (100×.)
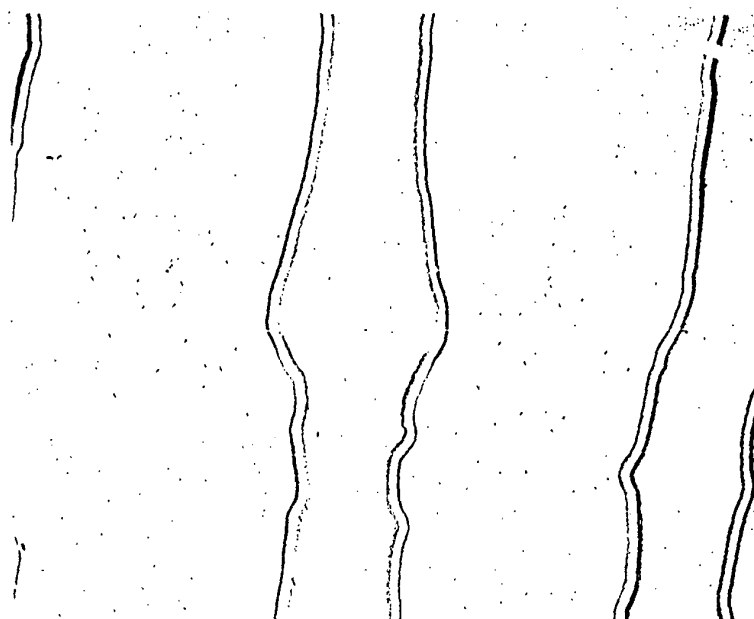
FIG. 5. Longitudinal section of a droplet trail in silicon with a medium dislocation density of 10^5 disl/cm². Trails in such material exhibit many relatively large random displacements perpendicular to the thermomigration direction. (200×.)

while those slightly off axis tend to be rounded. (Figs. 2 and 3).

The effect of dislocations on the mean square displacement of the droplets varies as the dislocation density changes. For low dislocation densities ($<5 \times 10^4$ disl/cm²), the mean square displacements are relatively small as might be anticipated. For medium dislocation densities (5×10^4 to 5×10^7 disl/cm²), the mean square displacement of the droplets is a maximum. Finally, the mean square displacement decreases with further increase in dislocation density and becomes relatively small again at high dislocation density (10^8 disl/cm²). Figures 4, 5, and 6 show respectively, metallographic stained longitudinal sections of droplet trails in crystals with dislocation densities of $\ll 5 \times 10^1$ disl/cm², 10^4 disl/cm², and 10^8 disl/cm² corresponding to the low, medium, and high dislocation ranges discussed above. Both the low and high dislocation density samples have relatively straight trails in comparison to the medium dislocation density sample whose trails exhibit many random displacements perpendicular to the thermal gradient trajectory of the trail. In all cases, the dislocation density in the doped silicon trail redeposited by the migrating droplet was found to be much less than the dislocation density in the surrounding silicon matrix. (Figs. 4—6) No dislocations or dislocation network was found at the doped trail-matrix interface as shown in Fig. 7.

No relationship was found between the magnitude of the random-walk displacement and the droplet size or the temperature. (Note, however, that for equal values of $\langle X^2 \rangle$, an optical illusion suggests that arrays of smaller droplets are more irregular than arrays of larger droplets.)

IV. DISCUSSION

In the discussion we will offer explanations for the following observations.

(1) The large random-walk displacements and faceting of droplets migrating along the $\langle 100 \rangle$ direction.

(2) The smaller random-walk displacements and rounding of droplets migrating slightly off the $\langle 100 \rangle$ direction.

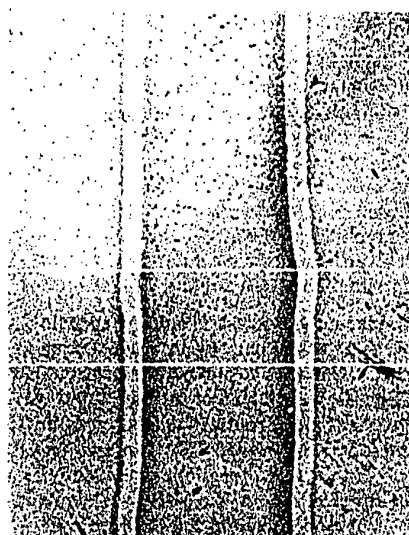

FIG. 6. Longitudinal section of a droplet trail in silicon with a high dislocation density. Trails in such material are straight. (250×.)

2319   J. Appl. Phys., Vol. 47, No. 6, June 1976

T.R. Anthony and H.E. Cline   2319

FIG. 7. Electron micrograph of $n-p$ junction formed by p-type trail left behind the migrating droplet in a n-type matrix. No dislocations or dislocation networks were found in the $p-n$ junction. (100 000×.)

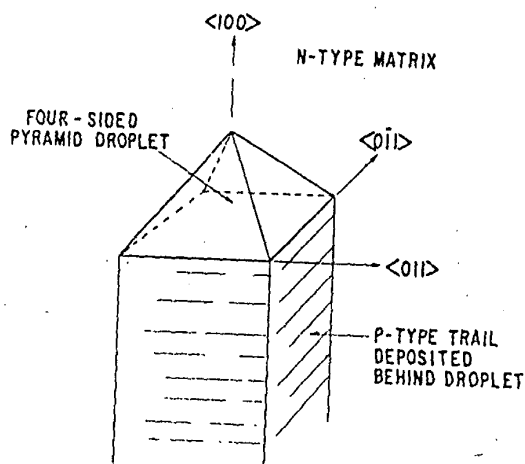(3) The effects of three ranges of dislocation densities.

(4) The low dislocation densities in the doped redeposited-silicon trails left behind the droplets.

A. Migration along the (100) direction

First, we will begin by calculating the random-walk displacements of droplets migrating exactly along the $\langle 100 \rangle$ direction. Aluminum-rich droplets migrating along the $\langle 100 \rangle$ direction in silicon are four-sided pyramids with the apex of the pyramid pointing forward in the $\langle 100 \rangle$ migration direction as shown schematically in Fig. 8.[5,6] An actual cross section along a $(0\bar{1}1)$ plane of some migrating droplets is shown in Fig. 9. Because of the droplet symmetry, we need only consider random displacements along either the $\langle 0\bar{1}1 \rangle$ for the $\langle 011 \rangle$ direction.

The random displacements S of a droplet perpendicular to the $\langle 100 \rangle$ droplet migration results when a droplet migrates through a dislocation forest. A dislocation that intersects one of the forward faces of migrating pyramidal droplet will cause preferential dissolution of this face. Because the forward faces of the pyramidal droplet are at an angle to the $\langle 100 \rangle$ direction, preferential dissolution of one forward face will cause a net displacement of the droplet perpendicular to the $\langle 100 \rangle$ migration direction (Fig. 10). In general, dislocation intersections with the forward faces will occur randomly as a droplet migrates through a crystal. The resulting random displacements of the droplet perpendicular to its migra-

FIG. 8. A perspective drawing of the pyramidal shape adopted by aluminum-rich droplets migrating along the (100) direction in silicon.

tion direction will cause a net mean square displacement of the droplet from its initial thermal trajectory after the droplet has migrated a given distance through the crystal.
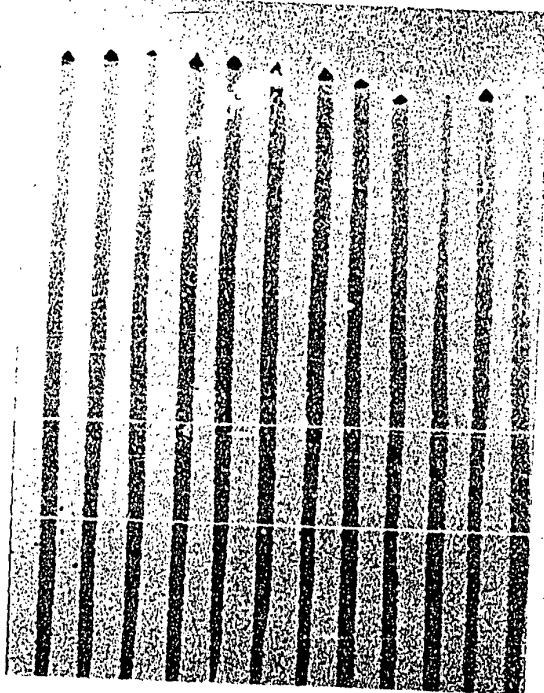
Consider a droplet that has already suffered a net

FIG. 9. A metallographic longitudinal cross section parallel to a (011) plane of a row of aluminum-rich droplets migrating in the (100) direction in silicon. (20×.)
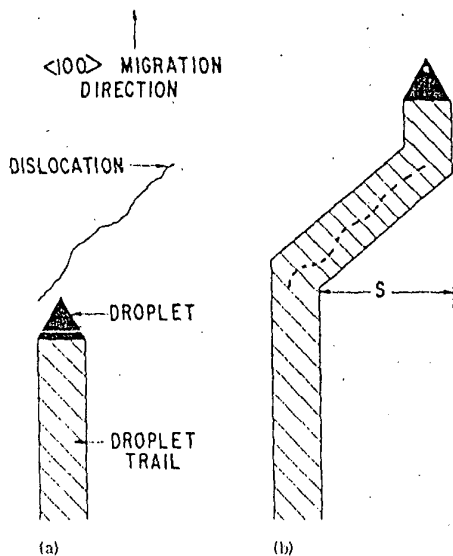
FIG. 10. The mechanism by which a preferential dissolution of a forward face induced by an intersecting dislocation causes a random-walk displacement S of a droplet perpendicular to the ⟨100⟩ migration direction.

displacement X_{N-1} because of $N-1$ previous dislocation intersections. The net displacement X_N after the Nth dislocation intersection is then

$$X_N = X_{N-1} + S, \tag{1}$$

where S is the displacement caused by the Nth dislocation. Squaring both sides,

$$X_N^2 = X_{N-1}^2 + 2X_N \cdot S + S^2. \tag{2}$$

The average random-walk displacement $\langle X_N^2 \rangle$ caused by N displacements resulting from N dislocation intersections is found by averaging the terms of Eq. (2).

$$\langle X_N^2 \rangle = \langle X_{N-1}^2 \rangle + \langle S^2 \rangle. \tag{3}$$

where the term $2X_{N-1} \cdot S$ averages to zero because there is no correlation between the net displacement X_{N-1} after $N-1$ random steps and the Nth displacement S. Iterating Eq. (3) (e.g., $\langle X_{N-1}^2 \rangle = \langle X_{N-2}^2 \rangle + \langle S^2 \rangle$; $\langle X_{N-2}^2 \rangle = \langle X_{N-3}^2 \rangle + \langle S^2 \rangle$) we find

$$\langle X_N^2 \rangle = N \langle S^2 \rangle, \tag{4}$$

where N is the number of times the droplet has been randomly displaced perpendicular to the thermal gradient by intersecting dislocations and $\langle S^2 \rangle$ is the mean square average of the variable length displacements S induced by the intersecting dislocations. $\langle X^2 \rangle$ can thus be calculated either from experimental measurements of N and $\langle S^2 \rangle$ from metallographic longitudinal sections of trails left behind the droplet (see Table II) or by calculating N and $\langle S^2 \rangle$ from theory.

Experimental measurements of N and $\langle S^2 \rangle$ result in a calculated value of $(\langle X^2 \rangle)^{1/2}$ of 1.70×10^{-2} cm as compared to an observed value of $(\langle X^2 \rangle)^{1/2}$ at the exit surface of 1.80×10^{-2} cm (Table II) for the first specimen in Table I.

TABLE II. The magnitude of the displacement steps S and the distance λ between displacement steps as observed directly in infrared transmission microscopy. Also, N, $\langle S^2 \rangle$, and $\langle X^2 \rangle$ calculated from this data are included.

	Magnitude of displacement step S (10^{-4} cm)	Distance from last displacement step λ (10^{-4} cm)
1	+ 60	550
2	− 40	100
3	+ 60	130
4	− 50	995
5	− 60	400
6	+ 50	1300
7	− 30	200
8	− 110	850
9	+ 10	300
10	− 10	700
11	+ 50	800
12	− 30	200
13	+ 10	200
14	− 10	200
15	+ 25	800
16	− 40	250
17	− 15	200
18	+ 20	350
19	+ 20	900
20	− 40	1000
21	+ 30	200
22	− 30	150
23	+ 50	950
24	− 20	400
25	− 20	200
26	+ 70	900
27	− 30	600
28	+ 40	200
29	− 70	200
30	+ 20	700
31	− 30	600
32	+ 40	200
33	− 70	200
34	+ 20	700
35	+ 10	450
36	+ 130	1000
37	+ 30	500
38	− 10	400
39	− 30	500
40	− 60	1000
41	+ 70	400
42	+ 150	900
43	− 70	1000
44	− 50	400
45	− 60	500
46	− 80	600
47	− 100	400
48	− 20	500
49	− 60	900
50	− 10	900
51	+ 50	300
52	− 50	200
53	+ 20	200
54	− 80	200
55	− 90	700
56	− 40	400
57	− 60	550
58	+ 70	600
59	+ 20	400

$\sum_i S_i^2 = 1.64 \times 10^{-3}$ cm^2

$\langle S^2 \rangle = 2.68 \times 10^{-5}$ cm^2

$(\langle X^2 \rangle_{obs})^{1/2} = 1.80 \times 10^{-2}$ cm

$\sum_i \lambda_i = 3.02$ cm

$\langle \lambda \rangle = 5.12 \times 10^{-2}$ cm

$N = 1/\langle \lambda \rangle$
$= 19.5$ displ/cm

$(\langle X^2 \rangle_{calc})^{1/2} = (N \langle S^2 \rangle)^{1/2}$
$= 1.7 \times 10^{-2}$ cm

2321   J. Appl. Phys., Vol. 47, No. 6, June 1976

T.R. Anthony and H.E. Cline   2321

<100> MIGRATION DIRECTION

DISLOCATION

DISLOCATION
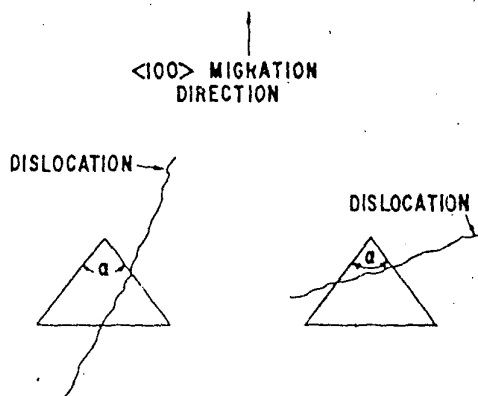
FIG. 11. Two-dimensional projection of pyramidal droplet migrating in the ⟨100⟩ direction. In (a), the dislocation line vector lies within the apex angle α of the droplet and only penetrates one forward face. In (b), the dislocation line vector lies outside the apex angle range α and thus penetrates two opposite forward faces.

If intersecting dislocations generate the observed random-walk displacements of migrating droplets, it is of interest to the technologist to model this phenomenon so that the *qualitative* effects of changes in such parameters as dislocation densities and droplet sizes can be predicted. With this limited goal in mind, we will make a rough estimation of $\langle X^2 \rangle$ from values of N and $\langle S^2 \rangle$ calculated from a simple two-dimensional model for various dislocation densities and droplet sizes. Using a two-dimensional model (and thus a droplet with only two forward faces), the number of random displacements N per unit migration length can be found from the number of separate times a migrating droplet has had a dislocation intersecting *only one* of its forward faces during a migration distance L. The line vector of a dislocation which intersects only *one* forward face of the droplet (see Figs. 8–10) must be at an angle such that it lies in the projected apex angle α of the pyramidal droplet [Fig. 11(a)]. Dislocations lines at other angles will intersect two opposing forward faces and will not lead to a net sideways displacement of the droplet. For pyramidal aluminum-rich liquid droplets in silicon bound by four (111) planes, the projected apex angle is about $\frac{1}{3}\pi$ so that only $\frac{1}{3}\pi/\pi = \frac{1}{3}$ of the dislocations that intersect a droplet will intersect only one forward face and thus lead to a displacement S of the droplet. During a migration distance L, the total number of dislocations that intersect a droplet is equal to the area $2BL$ swept out along the sides of the migrating droplet times the dislocation density ρ where B is the base width of the pyramidal droplet. Only about one-third of these intersecting dislocations intersect only *one* forward face and thus lead to net displacements in the one dimension that we are considering. Hence, the number of displacement steps N is equal to the density of single-face intersecting dislocations, $\frac{1}{3}\rho$, times the area $2BL$ swept out by along the sides of the migrating droplet for low dislocation densities.

$$N = \frac{2}{3}\rho BL, \quad \rho B^2 \ll 1. \tag{5}$$

For high dislocation densities $\rho B^2 \gg 1$, dislocations will always intersect both opposite forward faces so that none of the forward faces of the pyramidal droplet will dissolve faster than any other. Thus, no displacements will result so that N will approach zero at high dislocation densities.

$$N = 0, \quad \rho B^2 \gg 1. \tag{6}$$

Now let us calculate the average displacement S generated by a dislocation intersecting a single forward face for the case of small droplet sizes (as used in our experiments) and low dislocation densities ($\rho B^2 \ll 1$). Figure 12 shows a droplet being displaced sideways by a dislocation that intersects only one forward face of the droplet. The droplet will follow along the dislocation line since once the dislocation intersection reaches the forward apex of the droplet by sideways migration; forward-directed migration other than along the dislocation line will cause the dislocation intersection to move to the face where preferential dissolution on this face will cause the apex of the droplet to move back towards the dislocation line. Hence the droplet will tend to move along the dislocation line until it hits another dislocation.[14] If $\lambda = \rho^{-1/2}$ is the average spacing between dislocations, then the net displacement S caused by a dislocation at an angle θ with the thermal gradient is $\lambda \sin\theta$. The average mean square displacement $\langle S^2 \rangle$ is then,

$$\langle S^2 \rangle = \left(\int_{-\pi/6}^{\pi/6} \lambda^2 \sin^2\theta \, d\theta \right)\left(\int_{-\pi/6}^{\pi/6} \sin^2\theta \, d\theta \right)^{-1}$$

$$\approx 0.2\lambda^2 = 0.2\rho^{-1}, \tag{7}$$

where we have integrated only over those dislocations lines that lay within the apex of the pyramidal droplet and thus lead to displacements.

Substituting in values of N and $\langle S^2 \rangle$ from Eqs. (5) and (7) into Eq. (4), we find that the mean square displacement $\langle X^2 \rangle$ of a pyramidal liquid droplet with base length B migrating up a thermal gradient a distance L through a dislocation forest density ρ is for low dislocation densities

$$\langle X^2 \rangle = \frac{2}{3}(\rho BL)(0.2\rho^{-1}),$$
$$\langle X^2 \rangle = \frac{1}{10}BL, \quad \rho B^2 \ll 1 \tag{8}$$

which is independent of dislocation density in this dislocation density range. For high dislocation densities, we do not have to calculate $\langle S^2 \rangle$ since Eqs. (6) and (4) already show that

$$\langle X^2 \rangle \approx 0, \quad \rho B^2 \gg 1 \tag{9}$$

in agreement with our high dislocation density experiments (see Fig. 6). Unfortunately, most of our experiments were in a range which was not clearly either a very high or very low dislocation density range so that one would expect the measured values of $\langle X^2 \rangle$ to be in between the values given by Eqs. (8) and (9) as is observed.

An important ratio in technology is the ratio of the random-walk distance $(\langle X^2 \rangle)^{1/2}$ and the penetration distance L of the droplet into the material. For example, to make high resolution columnar diode arrays in silicon for imaging x rays or infrared,[5] this ratio must be small. From Eq. (9), it can be seen that this ratio will
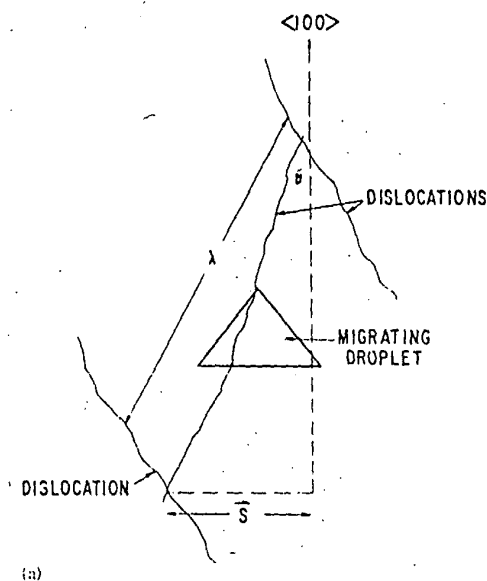
(a)
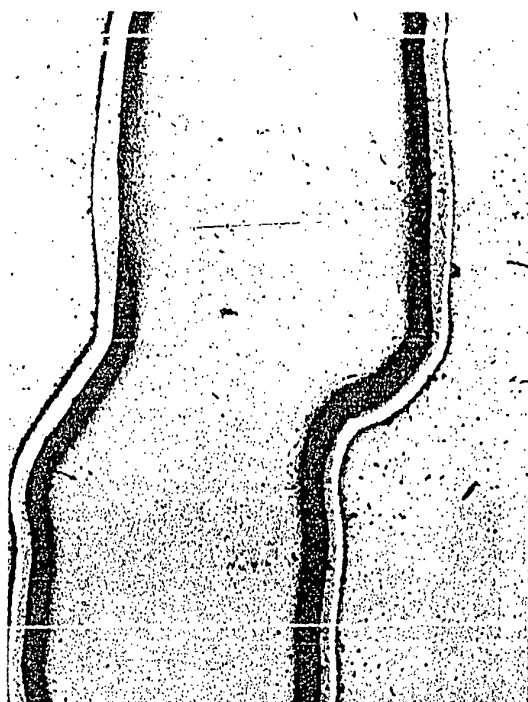
(b)

FIG. 12. (a) A droplet migrating through a dislocation forest showing the displacement S generated by a dislocation separated by a spacing λ. (b) A photomicrograph of a displacement produced in a droplet trail by dislocations. Note dislocation etch pits near the displacement step on either side of the droplet trail. (750×.)

be very small for high dislocation density silicon. For relatively low dislocation density silicon on the other-hand, Eq. (8) indicates that this ratio will be of the

order $(B/10L)^{1/2}$. Thus to minimize disregistry in columnar diode arrays in low dislocation silicon, one should use the sma... droplets possible.

B. Migration slightly off the (100) axis

If instead of aligning the thermal gradient parallel to the ⟨100⟩ direction, the thermal gradient is applied in a direction a few degrees off the ⟨100⟩ axis, the thermal gradient will favor the preferential dissolution of one forward face of the droplet because that face will be at a higher average temperature than the other forward faces. In the silicon-aluminum system as in most other systems, the preferential dissolution generated by a higher temperature will override the preferential dissolution produced by intersecting dislocations. Consequently the off-axis thermal gradient will override and prevent the *random* dislocation-induced sideways displacements of the droplet perpendicular to the ⟨100⟩ direction that occur when the thermal gradient is exactly along the ⟨100⟩ direction. Instead there will be a steady *nonrandom* displacement of the droplet perpendicular to the ⟨100⟩ axis in a direction dictated by the slightly off-axis thermal gradient.

The substitution of a *nonrandom* displacement for a random displacement is technologically important as it allows one to migrate large arrays of droplets through silicon without losing the original registry of the array. To maximize the preservation of the original registry, the off-axis component of the thermal gradient must have its sideways component in a ⟨010⟩ direction so that two of the four forward faces of the droplet are clearly favored for dissolution. Figure 13 looking down the ⟨100⟩ axis shows a droplet migrating toward the viewer in the ⟨100⟩ direction. With the sideways component of the off-axis thermal gradient along the ⟨010⟩ direction, faces I and II dissolve preferentially and produce a smooth nonrandom displacement of the droplet perpendicular to the ⟨100⟩ axis. If the off-axis component of thermal gradient is aligned in the ⟨011⟩ direction (see Fig. 13), random displacements would still be induced by dislocation intersections in the ±Y directions and would cause a disintegration of an initially registered array of migrating liquid droplets.

C. Morphology of the droplet trails

Droplets migrating exactly along the ⟨100⟩ direction leave faceted rectangular trail cross sections behind them [see Fig. 2(b)]. The reason that these trails are generally rectangular and not square is because of the
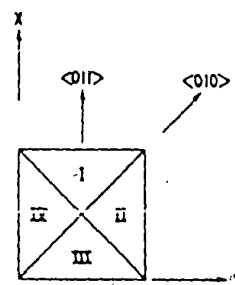

FIG. 13. A pyramidal aluminum-rich droplet migrating in a ⟨100⟩ direction in silicon. The forward four faces formed by (111) planes are shown in a view looking down the ⟨100⟩ axis. An off-axis component of the thermal gradient in the ⟨010⟩ direction will stop *random-walk* displacements of the droplet perpendicular to the ⟨100⟩ axis.

2323   J. Appl. Phys., Vol. 47, No. 6, June 1976

T.R. Anthony and H.E. Cline   2323

uneven dissolution of the four forward faces. If a dislocation threads through two opposing forward faces (e.g., faces I and III in Fig. 13), these faces will dissolve faster than the other pair of opposing faces (e.g., faces II and IV in Fig. 13) and will spread outward, causing the base of the droplet to change from a square to a rectangle [Fig. 2(b)].

The trails of droplets migrating in a slightly off-axis ⟨100⟩ direction appear rounded as can be seen in Fig. 1(b). The off-axis component of the thermal gradient was aligned in a ⟨010⟩ direction such that the forward two dissolving faces I and II in Fig. 13 remain flat because of dissolution faceting. In contrast, the trailing faces (faces III and IV in Fig. 13) have become curved because of deposition rounding[1-4] and are leaving behind a curved trail perimeter. The net result is a tear-drop trail cross section as can be seen in Fig. 1(b).

V. DISLOCATION DENSITY IN THE DROPLET TRAIL

Few if any dislocations are ever formed in the doped silicon trails left behind the migrating droplets. Thus the dislocation density in the droplet trails is generally much less than the dislocation density in the surrounding matrix. This result is not altogether unexpected since a slow even liquid epitaxy process (the crystal growth conditions in droplet migration) is known to be capable of depositing relatively low dislocation density material on even a high dislocation density substrate.

[1]T. R. Anthony and H. E. Cline, J. Appl. Phys. 42, 3380 (1971).
[2]H. E. Cline and T. R. Anthony, J. Appl. Phys. 43, 10 (1972).
[3]T. R. Anthony and H. E. Cline, Philos. Mag. 22, 893 (1970).
[4]H. E. Cline and T. R. Anthony, J. Appl. Phys. 43, 4391 (1972).
[5]W. G. Pfann, U.S. Patent 2,770,761 (1956).
[6]W. G. Pfann, U.S. Patent 2,813,048 (1957).
[7]T. R. Anthony and H. E. Cline, U.S. Patent 3,895,967 (1975).
[8]H. E. Cline and T. R. Anthony, U.S. Patent 3,898,106 (1975).
[9]H. E. Cline and T. R. Anthony, U.S. Patent 3,899,361 (1975).
[10]H. E. Cline and T. R. Anthony, U.S. Patent 3,899,362 (1975).
[11]T. R. Anthony and H. E. Cline, U.S. Patent 3,901,736 (1975).
[12]T. R. Anthony and H. E. Cline, U.S. Patent 3,902,925 (1975).
[13]T. R. Anthony and H. E. Cline, U.S. Patent 3,904,442 (1975).
[14]This approximation will overestimate the displacement S since the droplet may break away from an intersecting dislocation line before it runs into another dislocation because (1) the dislocation direction may change from a line direction that is effective to a line direction that is ineffective in causing a sideways displacement of the droplet; (2) the droplet is in some cases simultaneously pierced by two separate opposing dislocations whose effects cancel out; (3) the thermal gradient may pull the droplet away from an intersecting dislocation line before any appreciable sideways displacement occurs.